# Orientation Dependence of Laser Amorphization of Crystal Si

J. A. Yater and Michael O. Thompson

*Department of Materials Science, Cornell University, Ithaca, New York 14853*

(Received 8 May 1989)

Conditions for laser amorphization of Si were studied as a function of orientation for samples from [110] surface normal through [111] to [001] at 5° intervals. Two regimes of behavior are observed, one within 15° of [111] and a second for the remaining orientations. The transition energy density for amorphous-crystal regrowth and the maximum *a*-Si thickness change abruptly between regimes. These results are inconsistent with a single-ledge growth model and suggest that two separate interface morphologies or solidification mechanisms are active in the liquid-phase growth of Si.

PACS numbers: 61.50.Jr, 68.55.−a, 81.10.Fq

Numerous aspects of the behavior and structure of Si continue to defy understanding despite its technological importance and extensive research efforts. In particular, we are only now beginning to unravel the properties of the amorphous phase (*a*-Si). Amorphous Si is a dense random network but is not a true glass, i.e., not a thermodynamic extension of the liquid phase (*l*-Si). Rather, *a*-Si, a semiconductor with tetrahedral bonding, more closely resembles the normal crystalline phase (*c*-Si).[1,2] Previous work has shown that *a*-Si is a relatively well defined thermodynamic phase distinct from both *l*-Si and *c*-Si.[1]

Evidence for first-order transformations from *a*-Si to *c*-Si and *l*-Si are found in the sharp interfaces observed during solid-phase epitaxy (*a*-Si to *c*-Si) and during laser melting (*a*-Si to *l*-Si).[3,4] Even under ion-beam irradiation, the *c*-Si/*a*-Si interface remains sharp, further supporting first-order transitions.[5] The melting temperature of *a*-Si is estimated to be 1450 K, approximately 235 K below *c*-Si, from enthalpy measurements of the *c*-Si to *a*-Si transformations and direct measurements of *a*-Si melting.[1,6]

A unique metastable transformation from *l*-Si directly to *a*-Si bypassing the *c*-Si phase was reported a decade ago following picosecond laser melting of Si.[7] This laser-amorphized phase is not impurity stabilized and is thermally indistinguishable from *a*-Si formed by other techniques.[8] During laser irradiation, Si melts to a maximum depth determined by the laser fluence and pulse duration. Once molten, *l*-Si normally solidifies at a steady-state velocity and interface temperature determined by two criteria: (1) the interface response function relating the interface temperature and velocity and (2) heat-flow balance between conduction into the substrate and enthalpy release at the interface. Solidification into *a*-Si from *l*-Si occurs only under extremely high interface velocities and undercoolings. On a ⟨100⟩ *c*-Si/*l*-Si interface, *a*-Si forms for interface velocities exceeding $\approx 15$ m/s.[4] At this velocity, the interface must be undercooled to at least the *a*-Si melting point.[9] However, this is a lower bound only and kinetic or nucleation barriers may require additional undercooling.

The kinetics of *a*-Si formation are a sensitive probe of the nonequilibrium *c*-Si/*l*-Si interface but are poorly understood. In a series of nucleation experiments, *l*-Si supercooled 200 K below the *a*-Si melting temperature formed only *c*-Si.[10] Hence, during laser quenching, the *c*-Si/*l*-Si interface plays a central role and *a*-Si must nucleate at this interface despite being thermodynamically unfavorable. One model suggests that the *c*-Si/*l*-Si interface is intrinsically unstable to *a*-Si formation (much as a crystal/vapor interface is unstable to liquid formation) and *a*-Si forms as soon as the temperature drops below the thermodynamic limit.[11] Alternatively, interface morphological instabilities may act as the heterogeneous nucleation sites. Since both surface energies and the interface response function depend on the crystal orientation, variations in the amorphization conditions with orientation provide critical tests for these models.

We report the first detailed measurements of amorphization conditions as a function of the *c*-Si/*l*-Si growth-front crystallography. The transition energy for amorphization (and hence critical velocity) and the maximum *a*-Si thickness are reported between [110] and [001] surface orientations. Previously, the transition energies were only known at four orientations,[12] sufficient to identify differences but insufficient to discern details. The current results indicate two distinct regimes, and suggest that either amorphization or crystal growth undergoes a marked morphological change with orientation.

Wafers of Si were cut and polished from a single-crystal boule at 5° increments from the [110] surface normal through [111] to [001]. Samples were irradiated with spatially filtered 3-ns pulses from a frequency-quadrupled Nd-doped yttrium aluminum garnet laser ($\lambda = 266$ nm). The sample was translated between pulses so that each spot corresponded to a single melt and solidification cycle. A laser spatial filter (100-mm lens and 25-$\mu$m pinhole) removed energy variations with a period less than $\frac{1}{6}$ of the spot size, creating an energy profile varying approximately as a Gaussian in position.[13]

 © 1989 The American Physical Society

These irradiation conditions establish thermal gradients sufficiently steep to induce amorphous solidification. Each orientation was irradiated with peak energy densities from below melt threshold ($\approx 0.26$ J/cm$^2$) to near the surface damage threshold ($\approx 1.0$ J/cm$^2$). Samples were examined using Nomarski contrast optical microscopy, scanning electron microscopy, and a scanning reflectivity microscope to determine the surface structure and $a$-Si thicknesses. Under increasing laser energy (and hence decreasing solidification velocities), the surface morphology evolved from no melt, to melt with $a$-Si solidification, and finally to melt with $c$-Si regrowth. The energy dependence of $a$-Si formation on [100] and [111] orientations has been studied extensively[14] and the transition from $a$-Si solidification to $c$-Si regrowth occurs at a distinct energy density $E_c$ (dependent on orientation and irradiation parameters). Surface ripples, associated with melting by a coherent source, are observed at high energy densities. However, the ripples disappear at lower energies and could not be observed near the transition from $a$-Si to $c$-Si solidification.

The thicknesses of the $a$-Si were measured across the irradiated spots using a scanning reflectivity microscope with $a < 2$-$\mu$m spatial resolution. The reflectivity of a laser focused through a 20× microscope objective was monitored. This reflectance, determined by interference from the $a$-Si/$c$-Si and $a$-Si/air interfaces, was converted directly to an $a$-Si thickness. The periodic ambiguity was removed by monitoring the reflectivity at two wavelengths, 632 and 790 nm. The maximum $a$-Si thickness was determined by scanning directly across the transition from $a$-Si to $c$-Si solidification. Transmission electron microscopy[12] and ion-channeling techniques,[4] previously used to measure the $a$-Si thickness, do not provide adequate spatial resolution or selectivity.

The ratio of the energy density at the onset of crystallization, $E_c$, to that at the onset of amorphization, $E_a$, was determined by comparing surface morphologies at different incident energies. The Gaussian spatial variation of the beam results in well defined regions of $a$-Si and $c$-Si. At a low energy density, a unique region of $a$-Si growth was identified, with the boundary representing an energy contour at $E_a$. At a higher incident energy, this same contour separated regrown $c$-Si from surrounding $a$-Si, the border now marking a contour of $E_c$. The ratio of the incident laser energies accurately determines $E_c/E_a$. At each orientation, results from twenty to thirty irradiated spots were averaged; the error bars are the statistical variation. The $E_c/E_a$ ratios are plotted as a function of orientation in Fig. 1. The melt threshold is assumed equal to $E_a$ and independent of orientation (Si, with cubic symmetry, is isotropic to heat flow).

These energy-density measurements are closely related to the maximum melt depth and interface velocity. However, depths and velocities can only be obtained experimentally on (001) silicon on sapphire.[4] Using results obtained under slightly different conditions,[15] the maximum depth and velocity were estimated by scaling the energy densities to the melt threshold. The uncertainty in melt depth is $\approx \pm 10\%$, limited primarily by errors in the energy density. The velocity estimates, however, may be substantially in error since the orientation dependence of the interface response function is unknown.

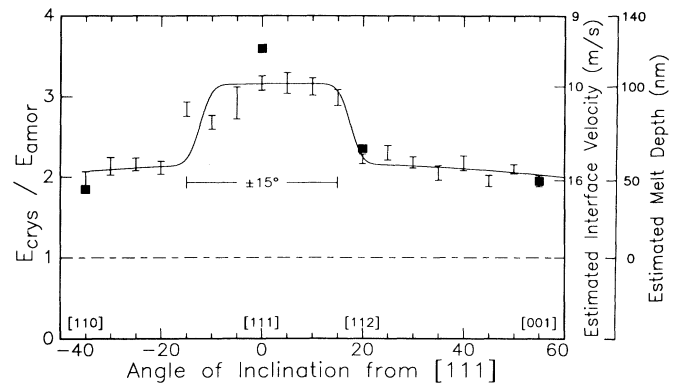


FIG. 1. Ratio of $E_c/E_a$ for oriented Si samples. Interface velocities and melt depths are estimates only. Square data points are from Cullis *et al.* (Ref. 12) at [110], [111], [112], and [001]. The $\pm 15°$ region about [111] is indicated.

These results agree with earlier data on [001], [110], [112], and [111] orientations.[12] In considering more orientations, however, there is clearly a discontinuity in behavior. The most striking feature of these data is the abrupt increase in $E_c/E_a$ for samples within 15° of [111]. Within the scatter, samples in this regime exhibit uniform behavior with $E_c/E_a \approx 3$ corresponding to an $a$-Si to $c$-Si transition at $\approx 10$ m/s in melts of 100 nm. Orientations near [001] and [110] also exhibit constant behavior, with $E_c/E_a \approx 2$ corresponding to velocities of $\approx 16$ m/s and maximum melt depths of 50 nm. These data suggest a sharp transition between two regimes with distinct solidification mechanisms.

Since amorphization near [111] continues to higher energy densities, the resulting $a$-Si layers are also thicker. However, the relationship between energy density (or peak melt depth) and the amorphous thickness has never been fully investigated. The $a$-Si thickness was measured across each irradiated spot, beginning in unmelted material, continuing through the $a$-Si and into the $c$-Si center [Figs. 2(a) and 2(b)]. Samples oriented within 15° of [111] again showed markedly different behavior from those near [001] and [110]. In all cases, the $a$-Si thickness increased steadily with increasing energy density until near the crystallization transition at $E_c$. In [111]-type samples, the $a$-Si thickness reaches a maximum at $E_c$, at the boundary between $a$-Si and $c$-Si. The $a$-Si thickness then drops sharply to zero within the $< 2$-$\mu$m resolution. In contrast, [001]- and [110]-type samples reach a peak $a$-Si thickness slightly below $E_c$, prior to the $c$-Si transition. Near $E_c$, the $a$-Si thickness decreases slightly before abruptly switching to $c$-Si.

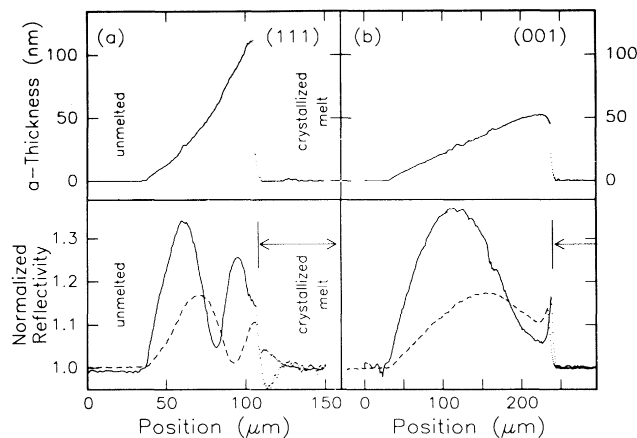


FIG. 2. (a) Reflectivity and corresponding $a$-Si thickness scan across [111] sample using 632-nm (solid line) and 790-nm source (dashed line). (b) Scans for [001] sample. Position scale corresponds to a monotonic, but not linear, increase in energy density.

For samples near [110] and [001], the reflectivity in the crystallized region equals the crystal value and exhibits no structure. However, samples within 15° of [111] exhibit additional structure due to defects in the $c$-Si near the boundary. Twin defects have previously been observed in Si for energy densities just above $E_c$ in [111] samples.[12] This reflectivity anomaly provides additional evidence for a fundamental difference in the solidification mechanism between the two regions.

Figure 3 summarizes the maximum-$a$-Si-thickness measurements. As in Fig. 1, an abrupt increase is observed for orientations within ≈15° of [111]. While samples near [111] consistently show $a$-Si thicknesses of 100–110 nm, the maximum $a$-Si thicknesses for samples oriented near [110] and [001] show a range of values from 30 to 70 nm. This scatter is well outside the measurement error. Such variations were observed both within a given spot and between spots, indicating fluctuations in the solidification process that are intrinsic to the $a$-Si formation in this regime.

The [001]-type samples exhibit behavior consistent with a velocity-controlled interface instability during $c$-Si growth. Once melt ceases, the velocity increases from zero to a steady-state value above some critical amorphization velocity. Crystalline regrowth occurs initially while the velocity increases to this amorphization velocity. As the energy density approaches $E_c$, the time required to reach the critical velocity increases and hence more of the melt solidifies as $c$-Si. The decreasing $a$-Si thickness near $E_c$ has not previously been observed because of the narrow energy range over which it occurs.

In contrast, the $a$-Si thickness in [111]-type samples increases continuously to a maximum at the transition, $E_c$. This peak $a$-Si thickness is, within the accuracy of the estimates, equal to the maximum melt thickness and

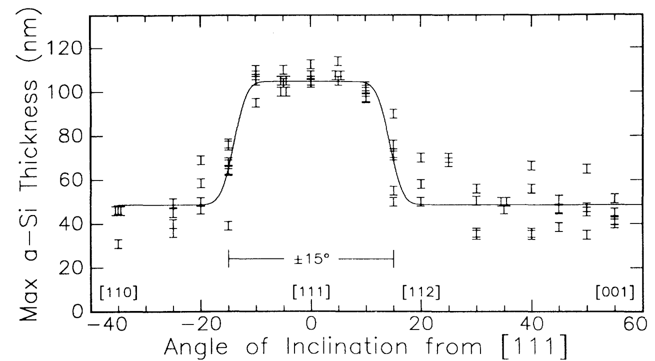


FIG. 3. Maximum $a$-Si thickness as a function of orientation. A region 15° to either side of [111] is identified. Each data point is a separate scan.

suggests that amorphization begins spontaneously just as the interface begins solidification. The absence of a region of decreasing $a$-Si thickness rules out a simple velocity-controlled instability and supports the absolute interface instability.

The amorphization process is closely coupled to the interface morphology and undercooling. In one model of solid-phase epitaxial crystallization of $c$-Si from $a$-Si, the advancing interface is bounded by planes normal to the slowest growth directions, the (111) planes.[9] Although the model is not directly applicable to this rapid liquid-phase growth, there is evidence that laser-induced solidification also occurs via lateral passage of {111} steps.[16] While such a model cannot reproduce the observed orientation dependence, it may explain the [111] region. We suggest that interfaces far from [111] are atomically rough and so solidify by collision-limited growth, while those near [111] are smooth and solidify via two-dimensional nucleation and ledge motion.[17] Evidence of such a structural difference has recently been seen in molecular-dynamics simulations of [100] and [111] $c$-Si growth using a Stillinger-Weber potential.[18] Insufficient data exist, though, to prove or disprove any such model and additional experimental interface probes are needed to identify the active growth mechanisms. The interfacial undercooling versus velocity, for example, should exhibit a similar dichotomy of behavior with orientation. Only [001] and [111] orientations have been measured at all though and only with relatively large errors.[19,20]

In conclusion, the orientation dependence of laser-induced amorphization of Si has been studied with unexpected results. Two regimes are observed, one operating within 15° of [111] and a second for remaining orientations. Near [111], $a$-Si solidification occurs for energies below $3E_a$ from near the maximum melt with $a$-Si thicknesses of 110 nm at $E_c$. Orientations near [110] and [001] represent the second regime with $a$-Si solidification occurring below $2E_a$ and maximum $a$-Si

thicknesses ranging from 30 to 70 nm. The *a*-Si thickness decreases slightly as the incident energy density approaches $E_c$.

The existence of the two regimes suggests two distinct solidification mechanisms. Behavior near [001] and [110] is consistent with a critical amorphization velocity, while results near [111] suggest an absolute interface instability. These results require reconsideration of the criteria for amorphization, specifically whether it can be tied to a particular velocity or temperature. While perhaps true for [001] and [110] orientations, the evidence does not support this conclusion for all orientations. These results represent a first step in developing a comprehensive microscopic understanding of laser amorphization dynamics.

We thank B. C. Larson and M. J. Aziz for the orientational samples, and M. J. Uttormark for simulation codes. This work is supported through the NSF-PYIA program (J. Hurt).

[1]E. P. Donovan, F. Spaepen, D. Turnbull, J. M. Poate, and D. C. Jacobson, Appl. Phys. Lett. **42**, 698 (1983).

[2]R. Zallen, *The Physics of Amorphous Solids* (Wiley, New York, 1983).

[3]L. Csepregi, E. F. Kennedy, T. J. Gallagher, J. W. Mayer, and T. W. Sigmon, J. Appl. Phys. **48**, 4234 (1977).

[4]M. O. Thompson, J. W. Mayer, A. G. Cullis, H. C. Webber, N. G. Chew, J. M. Poate, and D. C. Jacobson, Phys. Rev. Lett. **50**, 896 (1983); Michael O. Thompson, Ph.D. thesis, Cornell University, 1984 (unpublished), p. 167.

[5]J. Linnros and G. Holmen, J. Appl. Phys. **62**, 4737 (1987).

[6]M. O. Thompson, G. J. Galvin, J. W. Mayer, P. S. Peercy, J. M. Poate, D. C. Jacobson, A. G. Cullis, and N. G. Chew, Phys. Rev. Lett. **52**, 2360 (1984).

[7]P. L. Liu, R. Yen, B. Bloembergen, and R. T. Hodgson, Appl. Phys. Lett. **34**, 864 (1979).

[8]J. S. Custer, M. O. Thompson, and P. H. Bucksbaum, Appl. Phys. Lett. **53**, 1402 (1988).

[9]F. Spaepen and D. Turnbull, in *Laser Annealing of Semiconductors,* edited by J. M. Poate and J. W. Mayer (Academic, New York, 1982).

[10]S. R. Stiffler, M. O. Thompson, and P. S. Peercy, Phys. Rev. Lett. **60**, 2519 (1988).

[11]J. Y. Tsao and P. S. Peercy, Phys. Rev. Lett. **58**, 2782 (1987).

[12]A. G. Cullis N. G. Chew, H. C. Webber, and D. J. Smith, J. Cryst. Growth **68**, 624 (1984).

[13]The "bowl"-shaped melt puddle formed by a Gaussian beam inclines the liquid-solid interface slightly from the average surface orientation. This tilt is less than 0.5° in our geometry.

[14]J. M. Liu, Opt. Lett. **7**, 196 (1982).

[15]Heat-flow codes for uv irradiation are unreliable since optical constants are poorly known at high temperatures. Experimental data for the estimates were taken using 2.5-ns, 347-nm laser pulses. Using these data for our experimental conditions is reasonable since the effect of longer wavelength offsets the shorter pulse width.

[16]M. J. Aziz and C. W. White, Phys. Rev. Lett. **57**, 2675 (1986); L. M. Goldman and M. J. Aziz, J. Mater. Res. **2**, 526 (1987).

[17]M. J. Aziz (private communication).

[18]M. H. Grabow, G. H. Gilmer, and A. F. Bakker, in *Atomic Scale Calculations in Materials Science,* edited by J. Tersoff, D. Vanderbilt, and V. Vitek (Materials Research Society, Pittsburgh, 1989), p. 359.

[19]B. C. Larsen, J. Z. Tischler, and D. M. Mills, in *Fundamentals of Beam-Solid Interactions and Transient Thermal Processing,* edited by M. J. Aziz, L. E. Rehn, and B. Stritzker (Materials Research Society, Pittsburgh, 1988), p. 513.

[20]C. H. Galvin, J. W. Mayer, and P. S. Peercy, Appl. Phys. Lett. **46**, 644 (1985).